Quantum Electronics **51** (12) 1122–1126 (2021)

LASER BEAMS

https://doi.org/10.1070/QEL17658

Divergence features of laser beams with angular momentum

V.G. Niziev, A. Nesterov-Mueller

Abstract. **The physical features of the divergence of laser beams with angular momentum are investigated. The beams are presented in the form of a coherent superposition of two modes without angular momentum. Analytical formulas are used that satisfy Maxwell's equations for all components of the electric and magnetic fields of the initial modes. This allows one to describe the superposition of modes in terms of the components of the Umov–Poynting vector. The relationship between the beam divergence and its angular momentum, caused by the dependence of the radial and azimuthal components of the Umov–Poynting vector on the longitudinal components of the fields, is demonstrated. The components of this vector are analysed for an annular beam obtained using the superposition of azimuthally and radially polarised modes at various phase shifts between them. According to the analysis, beams with angular momentum can propagate without divergence. A method for generating such beams is discussed.**

Keywords: *divergence of laser beams, laser modes with angular momentum, radially and azimuthally polarised modes.*

1. Introduction

One of the fundamental differences between laser radiation and natural light is the low divergence of laser beams. Such parameters as the quality factor M^2 and beam parameter product (BPP) are used to estimate the divergence of a real laser beam in comparison with a Gaussian one [1]. Laser beam divergence is often a key parameter that determines its applicability in many applications. Divergence has a particular importance for the technological process carried out at a great distance from the radiation source [2], for remote sensing, for information transmission [3, 4], etc. The power density at an irradiated object depends linearly on the initial laser radiation power and quadratically on its angular divergence. Achieving the 'diffractive divergence' of a laser beam is the most important task in the development of various lasers [5–7].

The theoretical analysis of the angular divergence of a laser beam begins with the calculation of the radiation field distribution during beam propagation, and then the Umov–Poynting vector is calculated [8, 9]. A plane wave has no divergence, and its Umov–Poynting vector has one component along the z axis of wave propagation. In contrast, a diverging beam has a curved wavefront. A nonzero radial component of the Umov–Poynting vector appears in cylindrical coordinates. If the distributions of the longitudinal and radial components of this vector are known, the calculation of the beam divergence becomes a purely technical problem.

In a theoretical analysis of the propagation of a laser beam in space, two main approaches are used. The most famous theoretical method for determining the field distribution is the solution of Maxwell's equations. Usually the wave equation is solved in various approximations [10–12]. Successful attempts have also been made to overcome the limitations of scalar solutions that do not take into account the longitudinal components of the electric and magnetic fields [13, 14]. The second approach consists in solving diffraction problems using the Huygens–Fresnel principle [15], the Kirchhoff–Fresnel integral [16], or the Hertz vector [17]. Both approaches describe the propagation of typical laser beams with allowance for their divergence. However, the generalised form of such solutions does not make it possible to reveal the physical factors affecting the beam divergence.

For example, the physical reasons for the divergence of a Gaussian beam and a confined Bessel beam differ significantly. A Gaussian beam is an eigensolution of the scalar wave equation in free space. Its divergence is minimal for a finite beam size, and the field distribution during beam propagation remains Gaussian. The divergence of a Gaussian beam far from the waist is equal to the convergence of the beam produced by the focusing lens, which is typical for the geometric optics approximation. Diffraction phenomena play a special role in the waist region, where the beam radius is minimal. Here, a standing wave is formed in the radial direction, which determines the divergence of the beam behind the waist [18].

One of the scalar solutions to Maxwell's equations is a Bessel beam that has an infinite cross section; such a beam propagates without divergence. An aperture-limited Bessel beam is not such a solution. The field distribution during the propagation of this beam is not preserved, and diffraction restores the field beyond the aperture edges. Durnin et al. [19] discussed the features of the divergence of Bessel beams with a finite aperture. The intensity at the centre of the beam does not change until the process of diffractive 'decay' reaches the centre. The term 'diffraction free beams' is incorrect for such beams.

The classical Laguerre–Gaussian modes TEM_{pq} (p and q are the radial and azimuthal indices) can be observed during

V.G. Niziev Institute on Laser and Information Technologies, Branch of the Federal Scientific Research Centre 'Crystallography and Photonics', Russian Academy of Sciences, ul. Svyatoozerskaya 1, 140700 Shatura, Moscow region, Russia; e-mail: niziev@yahoo.com;
A. Nesterov-Mueller Karlsruhe Institute of Technology, Hermann-von-Helmholtz-Platz 1, D-76344 Eggenstein-Leopoldshafen, Germany; e-mail: alexander.nesterov-mueller@kit.edu

Received 24 September 2021
Kvantovaya Elektronika **51** (12) 1122–1126 (2021)
Translated by I.A. Ulitkin

lasing in cavities with circular mirrors. The field distributions of these modes are solutions to the scalar wave equation under the assumption of uniform linear polarisation in the beam cross section [11, 20]. Along with the classical modes, Kogelnik and Li [11] observed some other modes, which are formed as a result of the coherent superposition of classical modes. Later, these modes, for example, with azimuthal and radial polarisations, found a fairly wide application in technology and various studies [21]. The divergence of beams with such a field distribution was not specially investigated, since there was no reason to assume that there are significant differences from the case of ordinary modes.

In recent years, laser beams with spin [22] or orbital [23] angular momentum have attracted great interest due to the possibility of their use for trapping and moving micro- and nanoparticles or for transmitting information. In particular, Ustinov et al. [24] investigated the generation of laser beams with angular momenta of both types, with the total angular momentum being equal to zero. The divergence of such beams did not attract attention. This work is devoted to the study of the divergence of laser beams with angular momentum. The calculations were performed for modes with circular symmetry of all parameters, including polarisation.

2. Physical principles and calculation methods

The properties of laser beams are equally determined by both electric and magnetic radiation fields. Six field components are described by Maxwell's system of equations. We will use all these components for the analysis. The fields of the electromagnetic wave and the practically measured parameters of the laser beam are related using three components of the Umov–Poynting vector $\boldsymbol{S} = \boldsymbol{E} \times \boldsymbol{H}$.

Time-averaged z-component (along the beam axis) of the Umov–Poynting vector

$$\boldsymbol{S}_z = \boldsymbol{S}_{z1} + \boldsymbol{S}_{z2} \propto (E_r H_\varphi - E_\varphi H_r)\boldsymbol{e}_z \tag{1}$$

describes the transfer of energy in the direction of propagation of an electromagnetic wave. The radially directed component

$$\boldsymbol{S}_r = \boldsymbol{S}_{r1} + \boldsymbol{S}_{r2} \propto (E_\varphi H_z - E_z H_\varphi)\boldsymbol{e}_r \tag{2}$$

is associated with the beam divergence. The azimuthally directed component

$$\boldsymbol{S}_\varphi = \boldsymbol{S}_{\varphi 1} + \boldsymbol{S}_{\varphi 2} \propto (E_r H_z - E_z H_r)\boldsymbol{e}_\varphi \tag{3}$$

is responsible for the formation of the angular momentum of the beam. For further calculations in a cylindrical coordinate system, the field components and the Umov–Poynting vector are conveniently represented in the form of a diagram shown in Fig. 1. The field components are at the vertices of the hexagon. A feature of this representation is that when calculating the components of the Umov–Poynting vector, a nontrivial result can be obtained in the case of multiplying any field component by only two adjacent components.

Next, we turn to work [18], where it was shown that a necessary condition for the divergence of the beam far from the waist region is the presence of a standing wave in it (Fig. 2). Consider an axially symmetric laser beam. After the beam passes through the lens, the Umov–Poynting vectors are

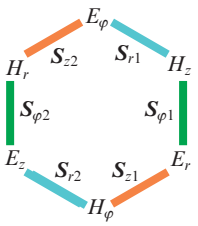

Figure 1. (Colour online) Graphical representation of the components of the electric and magnetic fields and the components of the Umov–Poynting vector.

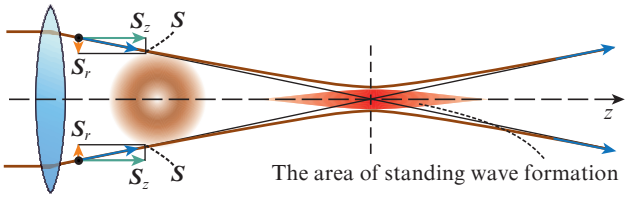

Figure 2. (Colour online) Circular Laguerre–Gaussian mode focused by a lens. The components of the Umov–Poynting vector S_r and S_z are shown. A standing wave is formed in the waist region.

directed at an angle to each other. They can be represented in the form of two components: longitudinal components equally directed along the beam axis and radial components directed perpendicular to the axis. The radially directed pulse generated by the lens does not disappear. The counterpropagating waves associated with these radial components of the Umov–Poynting vector interfere in the focal region, producing a standing wave during their interaction. The maximum value of the field amplitude of such a wave is observed in the waist region. Travelling waves that have formed a standing wave continue to move. After the beam passes through the waist region, the radial components of the Umov–Poynting vector are directed from the beam axis, which leads to the beam divergence. This process is consistent with Maxwell's equations and, in particular, satisfies the reciprocity principle.

3. Superposition of azimuthally and radially polarised modes with different phase shifts

Complete vector analysis using the lowest-order modes with azimuthal and radial polarisations is representative and informative. If these modes are combined coherently, then different mode structures are obtained depending on the phase shift of the initial modes. Figure 3 shows two cases of superposition of modes with different phase shifts: $\Delta\chi = 0$ и $\pi/2$. In the first case (Fig. 3a), the result of superposition is a linearly polarised mode with the same angle between the field vector and the radius vector at each point of the beam cross section. The superposition of modes in Fig. 3b is a circularly polarised mode with angular momentum.

The resulting modes are convenient for analysis, since there are analytical solutions for all field components of the initial modes that satisfy Maxwell's equation in the paraxial approximation $\nabla \boldsymbol{F} = 0$ ($\boldsymbol{F} = \boldsymbol{E}, \boldsymbol{H}$). For the vector description of each of the two initial modes, only three field components are required (H_φ, E_r, E_z and E_φ, H_r, H_z), with the other three components being equal to zero. The solution of the vector

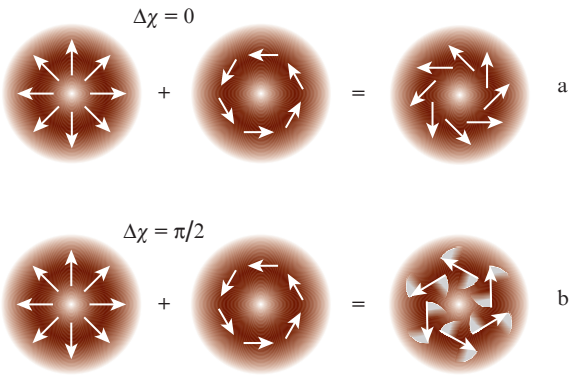

Figure 3. (Colour online) Superpositions of radially and azimuthally polarised modes with phase shifts Δχ = (a) 0 and (b) π/2. For Δχ = 0, the polarisation is linear at all points of the cross section of the resulting mode, and for Δχ = π/2, it is circular. This illustrates the 'tail' from the rotation of the field vector.

wave equation for a mode with an azimuthally directed field vector (electric or magnetic) is a one-component solution with circular symmetry [25, 26]:

$$E_\varphi = H_\varphi = \left(\frac{2}{\sqrt{\pi}}\frac{1}{w}\right) R\exp(-R^2)\exp(\mathrm{i}\theta) \times \exp[\mathrm{i}(\omega t - kz)], \tag{4}$$

where

$$\theta = 2\arctan Z - ZR^2; \quad R = \frac{r}{w}; \quad \frac{w^2}{w_0^2} = (1+Z^2); \quad Z = \frac{z}{z_0}; \quad z_0 = \frac{\pi w_0^2}{\lambda}; \tag{5}$$

and w_0 is the beam waist radius. The solution for the azimuthal field in the waist ($z = 0$, $w = w_0$) is written in the form

$$E_\varphi = H_\varphi = \Omega\exp(\mathrm{i}\omega t), \tag{6}$$

where

$$\Omega(R) = \zeta R\exp(-R^2); \quad \zeta = \frac{2}{\sqrt{\pi}}\frac{1}{w_0}.$$

The radial and z-components for each of the two modes are calculated by the formulae

$$\boldsymbol{H} = \frac{\mathrm{i}}{k}(\nabla\times\boldsymbol{E}), \quad H_r = -\Omega\exp(\mathrm{i}\omega t), \quad H_z = \mathrm{i}\Psi\exp(\mathrm{i}\omega t),$$
$$\boldsymbol{E} = -\frac{\mathrm{i}}{k}(\nabla\times\boldsymbol{H}), \quad E_r = \Omega\exp(\mathrm{i}\omega t), \quad E_z = -\mathrm{i}\Psi\exp(\mathrm{i}\omega t), \tag{7}$$

where

$$\Psi(R) = \vartheta\frac{1}{R}\frac{\partial}{\partial R}(R\Omega) = 2\zeta\vartheta(1-R^2)\exp(-R^2); \quad \vartheta = \frac{1}{k}\frac{1}{w_0}. \tag{8}$$

To obtain expressions (7), we used the following intermediate calculations:

$$\nabla\times\boldsymbol{F}_\varphi = -\frac{\partial F_\varphi}{\partial z}\boldsymbol{e}_r + \frac{1}{r}\frac{\partial(rF_\varphi)}{\partial r}\boldsymbol{e}_z, \quad \boldsymbol{F}_\varphi = \boldsymbol{E}_\varphi(r,z),\ \boldsymbol{H}_\varphi(r,z),$$
$$\left|\frac{\partial F_\varphi}{\partial z}\right|_{z=0} \approx -\mathrm{i}k\Omega\exp(\mathrm{i}\omega t), \quad \frac{1}{r}\frac{\partial}{\partial r}(rF_\varphi)\Big|_{z=0} = \frac{1}{w_0}\left[\frac{1}{R}\frac{\partial}{\partial R}(R\Omega)\right]\exp(\mathrm{i}\omega t). \tag{9}$$

Real and imaginary terms in (7) describe oscillations with a phase shift π/2 [18].

The complex form of expression (7) is inconvenient for calculating the components of the Umov–Poynting vector, since we are considering the multiplication of the field components taking into account their phase shift. The phase shift π/2 has an important physical meaning. If the field components with a phase shift π/2 are multiplied, then the time-averaged Umov–Poynting vector describing the energy transfer is equal to zero [27]. However, when calculating the S_r component, such a phase shift is indicative of the presence of a standing wave, which 'decays' into travelling waves directed from the beam axis after it passes through the waist region, thereby forming a diverging beam. In order not to lose the primary information about the standing wave, we use the trigonometric form of the field components, calculating them from (7)–(9) with the help of formulae $\mathrm{Re}[\exp(\mathrm{i}\omega t)] = \cos(\omega t)$ and $\mathrm{Re}[\mathrm{i}\exp(\mathrm{i}\omega t)] = -\sin(\omega t)$.

Complete information about the initial modes, including their general form, all field components and components of the Umov–Poynting vector, is presented in Fig. 4. Each of the two modes has only three nonzero field components. The components of the Umov–Poynting vector for both beams are the same and have the following physical meaning:

– The time-averaged z-component is nonzero ($\bar{S}_z \neq 0$). Energy is transferred in the direction of beam propagation.

– Nonzero oscillations of the radial component S_r in the absence of energy transfer in the radial direction ($\bar{S}_r = 0$) indicate the presence of a standing wave. After the beam passes through the waist region, the standing wave decays, forming a diverging beam.

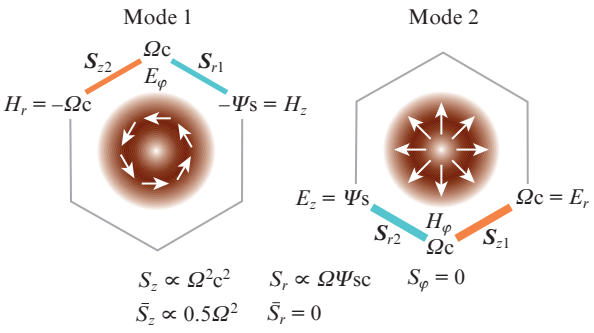

Figure 4. (Colour online) Graphical representation of the initial beams with azimuthal and radial polarisations: modes 1 and 2 with the corresponding field components and the Umov–Poynting vector. The formulae for the components of this vector are given below. Here, as in Figs 5–7, the letter s is used for sin(ωt) and the letter c for cos(ωt).

– The beams have no angular momentum, because $S_\varphi = 0$. The necessary field components are simply absent.

The superposition of these modes with a zero phase shift is shown in Fig. 5. The result of this superposition has the following features:
– Energy is transferred along the beam axis ($\bar{S}_z \neq 0$).
– A standing wave is formed in the waist for the r-component of the Umov–Poynting vector ($S_r \neq 0$, $\bar{S}_r = 0$).
– There are field components necessary for the formation of the angular momentum, which is equal to zero, since, according to (3), $S_\varphi = 0$.

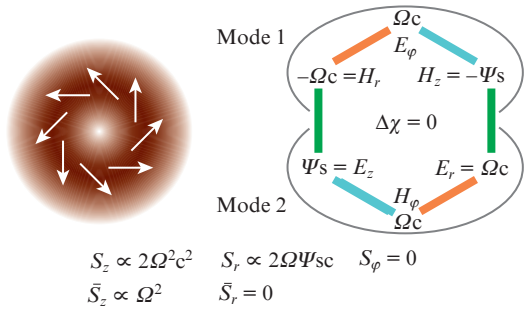

Figure 5. (Colour online) Superposition of modes 1 and 2 (Fig. 4) with a zero phase shift. The components of the fields and the Umov–Poynting vector are shown on the right.

The considered version of superposition does not give qualitative changes in comparison with the original modes. It is easy to verify that the superposition of two initial modes with a phase shift π does not lead to any qualitatively new results. The superposition of two modes (1 and 2) with a phase shift π/2 is the most interesting case (Fig. 6). With such a phase shift, the field components of mode 2 undergo the following obvious changes: $\sin(\omega t + \pi/2) = \cos(\omega t)$ and $\cos(\omega t + \pi/2) = -\sin(\omega t)$. In this case, the resulting mode has several special properties:
– The standing wave is absent ($S_r = 0$), which presumably indicates the absence of beam divergence after the waist.
– A nonzero azimuthally directed component of the Umov–Poynting vector indicates the appearance of angular momentum, which is directly proportional to the S_φ component.
– Nonzero components S_φ и and S_z do not oscillate in time; time averaging is not required.

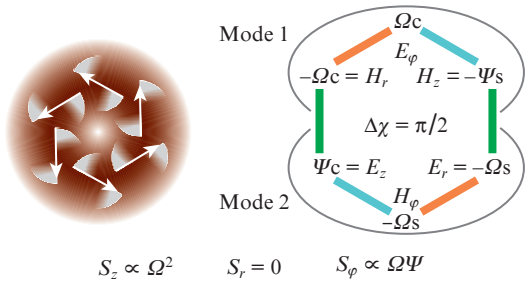

Figure 6. (Colour online) Superposition of modes 1 and 2 (Fig. 4) with a phase shift π/2 and the components of the Umov–Poynting vector of the resulting mode.

4. Discussion

A characteristic feature of the divergence of the Laguerre–Gaussian mode without angular momentum is the presence of a standing wave in the waist region. In the case of a superposition of modes 1 and 2 (Fig. 4) with a quarter-wave phase shift, the energy flux in the radial direction is completely absent in the presence of angular momentum (Fig. 7). The time-averaged radial component of the Umov–Poynting vector is always zero at the waist. However, in this case, the oscillating part of the radial component of this vector is also equal to zero, which indicates the absence of a standing wave, and hence the absence of beam divergence after its passage through the waist region. This beam is a nonoscillating spiral flux of light energy through the waist, since the nonzero components S_φ и and S_z do not oscillate in time, and the S_r component is completely absent. It should be noted that the calculations were performed for a mode with unique parameters. The methods for generating such a beam are not associated with any 'external influences' on its structure (finite aperture or any other obstacle). The fields of the investigated beam satisfy Maxwell's equations, have circular symmetry, and are described by relatively simple analytical solutions. The total angular momentum of the beam is zero.

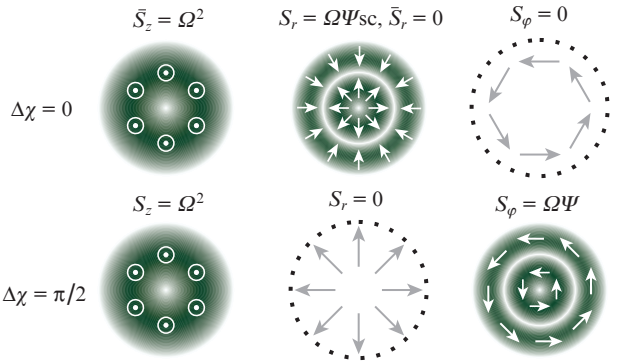

Figure 7. (Colour online) Results of calculating the radial dependences of the components of the Umov–Poynting vector for two cases of superposition of modes: at a zero phase shift, as in Fig. 5 (top), and at a phase shift π/2, as in Fig. 6 (bottom).

As far as we know, the Laguerre–Gaussian mode with this field structure and angular momentum, shown in Fig. 6, has not yet been experimentally realised. However, modern technologies make it possible to plan the generation of such modes. The simplest scheme consists of two stages. The first is the generation of an azimuthally polarised mode. There are different ways to obtain it [21]. At the second stage, a π/2 phase shifter is used based on a spiral relief pattern with a period shorter than the radiation wavelength [28, 29]. In this case, the period of the structure is inhomogeneous along the radius. An alternative solution (Fig. 8) is to rotate the field vector of the azimuthally polarised beam by 45° using conventional half-wave phase shifters [30]. Then, using a π/2 phase shifter with a relief pattern in the form of concentric circles with a constant step along the radius (Fig. 8d), a mode with angular momentum is formed.

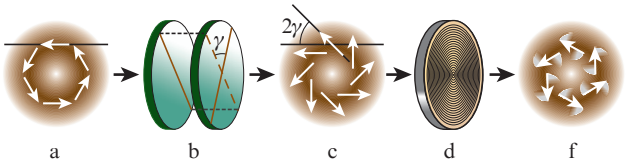

Figure 8. (Colour online) Schematic of optical elements for generating a mode with angular momentum. An azimuthally polarized laser beam (a) passing through a pair of phase shifters λ/2 (b) acquires an intermediate polarisation state (c). The π/2 phase shifter based on an annular diffraction grating (d) generates a laser beam with circular polarisation and angular momentum (e).

It is well known that radially (R-TEM$_{p1*}$) and azimuthally (A-TEM$_{p1*}$) polarised modes can be represented as a superposition of the classical linearly polarised Laguerre–Gaussian modes TEM$_{p1}$ mentioned in the Introduction. (An asterisk in the subscript means that the desired mode is obtained with the corresponding mutual orientation of the initial modes and a zero phase shift.) In this work, the calculations are presented for the lowest order mode (p = 0) with circular polarisation (C-TEM$_{01*}$). The scheme of its formation can be written as follows: R-TEM$_{01*}$ + A-TEM$_{01*}$ → C-TEM$_{01*}$ (Fig. 3b). It can be shown that the conclusions drawn for the C-TEM$_{01*}$ mode are also valid, in a more general case, for the higher-order C-TEM$_{p1*}$ modes.

An exhaustive description of the fields on a given surface, including in the beam cross section (in our case, in the waist), determines its further propagation. Integral methods are usually used for such a description, for example, the Kirchhoff–Fresnel integral [16]. However, these methods do not take into account the longitudinal field component in the original cross section. In this case, this is unacceptable. Longitudinal field components play an important role in the formation of angular momentum and divergence.

The presence of angular momentum is not a sufficient condition for the absence of divergence. For example, a beam with a spiral wavefront, the so-called spiral mode with uniform linear polarisation [23] and orbital angular momentum, also diverges according to similar calculations.

5. Conclusions

The study of the divergence of a laser beam with angular momentum has required a rethinking of the well-known concept, which considers such beams as a superposition of two modes without angular momentum. The new approach used a full set of analytical formulae for six field components that satisfied Maxwell's equations. The calculations have been performed using the example of the superposition of azimuthal and radially polarised modes. Superpositions of these modes at different phase shifts are fundamentally different, which follows from an analysis of the calculated components of the Umov–Poynting vector.

A convenient graphical method for representing the field components and the Umov–Poynting vector has been proposed. The divergence of laser beams with angular momentum has been analysed based on all three components of the Umov–Poynting vector in the waist. It has been shown that the considered beam with angular momentum can propagate without divergence, since the radial component of the Umov–Poynting vector is equal to zero. For beams without angular momentum, this component always exists and oscillates at doubled frequency. Another feature of this beam is that the nonzero components of the Umov–Poynting vector – azimuthal and longitudinal – do not oscillate in time.

References

1. *Lasers and Laser-Related Equipment – Test Methods for Laser Beam Widths, Divergence Angles and Beam Propagation Ratios* (ISO Standard 11146, 2005).
2. Vostrikov V.G., Gavrilyuk V.D., Krasyukov A.G., Naumov V.G., Svotin P.A., Shashkov V.M., Shachkin L.V., Demin V.M., Matveev S.N., Blokhin O.A., Yakovenko N.A. *Chem. Pet. Eng.*, **37**, 308 (2001).
3. Pearlman M.R., Degnan J.J., Bosworth J.M. *Adv. Space Res.*, **30**, 135 (2002).
4. Hu Z., Liu H., Xia J., He A., Du Z., Li Y., Li Z., Chen T., Li H., Lü Y. *J. Opt. Soc. Am. A*, **37**, 1404 (2020).
5. Agroskin V.Ya., Bravyi B.G., Vasil'ev G.K., Gur'ev V.I., Karel'skii V.G., Kashtanov S.A., Makarov E.F., Sotnichenko S.A., Chernyshev Yu.A. *Quantum Electron.*, **46**, 703 (2016) [*Kvantovaya Elektron.*, **46**, 703 (2016)].
6. Panchenko Yu.N., Losev V.F., Dudarev V.V. *Quantum Electron.*, **38**, 369 (2008) [*Kvantovaya Elektron.*, **38**, 369 (2008)].
7. Afonin Yu.V., Golyshev A.P., Ivanchenko A.I., Malov A.N., Orishich A.M., Pechurin V.A., Filev V.F., Shulyat'ev V.B. *Quantum Electron.*, **34**, 307 (2004) [*Kvantovaya Elektron.*, **34**, 307 (2004)].
8. Bekshaev A.Ya. *Proc. SPIE*, **3904**, 131 (1999).
9. Mafusire C., Krüger T.P.J. *J. Opt.*, **20**, 065603 (2018).
10. Goubau G., Schwering F. *IEEE Trans. Antennas Propag.*, **9**, 248 (1961).
11. Kogelnik H., Li T. *Appl. Opt.*, **5**, 1550 (1966).
12. Siegman A. *Lasers* (Mill Valley: University Science Books, 1986).
13. Lax M., Louisell W.H., Knight W.B. *Phys. Rev. A*, **11**, 1365 (1975).
14. Cicchitelli L., Hora H., Postle R. *Phys. Rev. A*, **41**, 3727 (1990).
15. Born M., Wolf E. *Principles of Optics* (Cambridge University Press, 1999).
16. Woan G. *The Cambridge Handbook of Physics Formulas* (Cambridge University Press, 2010).
17. Nesterov A.V., Niziev V.G. *Phys. Rev. E*, **71**, 046608 (2005).
18. Niziev V., Muys P. *J. Opt. Soc. Am. A*, **37**, 1839 (2020).
19. Durnin J., Miceli J.J., Eberly J.H. *Phys. Rev. Lett.*, **58**, 1499 (1987).
20. Svelto O. *Principles of Lasers* (New York: Plenum Press, 1998).
21. Zhan Q. *Adv. Opt. Photon.*, **1**, 1 (2009).
22. Beth R. *Phys. Rev.*, **50**, 115 (1936).
23. Allen L., Beijersbergen M.W., Spreeuw R.J.C., Woerdman J.P. *Phys. Rev. A*, **45**, 8185 (1992).
24. Ustinov A.V., Niziev V.G., Khonina S.N., Karpeev S.V. *J. Mod. Opt.*, **66**, 1961 (2019).
25. Nesterov A.V., Niziev V.G. *J. Phys. D: Appl. Phys.*, **33**, 1817 (2000).
26. Nesterov A.V., Niziev V.G. *J. Opt. B: Quantum Semiclassical Opt.*, **3**, 215 (2001).
27. Landau L.D., Lifshitz E.M. *The Classical Theory of Fields* (Oxford: Butterworth-Heinemann, 1980; Moscow: Nauka, 1988).
28. Bomzon Z., Kleiner V., Hasman E. *Opt. Lett.*, **26**, 1424 (2001).
29. Niv A., Biener G., Kleiner V., Hasman E. *Opt. Commun.*, **251**, 306 (2005).
30. Nesterov A.V., Niziev V.G. *J. Phys. D: Appl. Phys.*, **32**, 1455 (1999).